Earthquakes and Structures, *Vol. 15, No. 5 (2018) 499-511*
DOI: https://doi.org/10.12989/eas.2018.15.5.499

Experimental study on seismic behavior of RC beam-column joints retrofitted using prestressed steel strips

Yong Yang[a], Yang Chen[*], Zhan Chen[b], Niannian Wang[c] and Yunlong Yu[d]

School of Civil Engineering, Xi'an University of Architecture & Technology, Xi'an, Shaanxi 710055, China

(Received July 13, 2018, Revised August 14, 2018, Accepted September 5, 2018)

Abstract. This paper aims to investigate the seismic performance of the prestressed steel strips retrofitted RC beam-column joints. Two series of joint specimens were conducted under compression load and reversed cyclic loading through quasi-static tests. Based on the test results, the seismic behavior of the strengthened joints specimens in terms of the failure modes, hysteresis response, bearing capacity, ductility, stiffness degradation, energy dissipation performance and damage level were focused. Moreover, the effects of the amount of the prestressed steel strips and the axial compression ratio on seismic performance of retrofitted specimens were analyzed. It was shown that the prestressed steel strips retrofitting method could significantly improve the seismic behavior of the RC joint because of the large confinement provided by prestressed steel strips in beam-column joints. The decrease of the spacing and the increase of the layer number of the prestressed steel strips could result in a better seismic performance of the retrofitted joint specimens. Moreover, increasing the axial compression ration could enhance the peak load, stiffness and the energy performance of the joint specimens. Furthermore, by comparison with the specimens reinforced with CFRP sheets, the specimens reinforced with prestressed steel strips was slightly better in seismic performance and cost-saving in material and labor. Therefore, this prestressed steel strips retrofitting method is quite helpful to enhance the seismic behavior of the RC beam-column joints with reducing the cost and engineering time.

Keywords: reinforced concrete structure; beam-column joint; retrofitted methods; prestressed steel strips; experimental study; seismic performance

1. Introduction

The beam-column joints are the most critical members in reinforced concrete frame structure, which carry the large vertical and horizontal force and guarantee the integrity of the frame structure. A large number of post-earthquake investigations showed that the collapses of most of the existing reinforced concrete structures in earthquake were caused by the failure of the beam-column joints due to the improper design and construction as well as the inadequate material strength (Alemdar and Sezen 2010, Duan and Hueste 2012, Han 2016, Men 2015, Özgür 2015, Tsonos 2010, Khalili *et al*. 2016). Consequently, for moderately damaged buildings after earthquake attack, if those buildings are to be demolished, it will not only lead to environmental pollution, but also bring about waste of resources. And furthermore, for many old buildings built in early years, especially for those weak joints with low concrete strength or insufficient lateral stirrups configuration, their seismic performance and safety must be fully concerned. Thus, in order to ensure the safety of the old reinforced concrete buildings or the moderately damaged buildings, some appropriate measures have to be taken to enhance the overall seismic behavior of the joints.

Nowadays, there are many different retrofitting methods to strengthen the structural buildings, such as the enlarging section method (Guo 2011, Huang *et al*. 2012), the steel plate bonding method (Shan 2010, Tomatsu 1996) and externally bonded fiber-reinforced polymer composites method (Hawileh *et al.* 2014, Lee and Lopez 2016, Li 2015, Thomsen 2004, Wang 2010). Among these retrofitting methods, the method of wrapping carbon fiber reinforced plastics (CFRP) on the components surface was the most extensively studied (Aiello and Ombres 2004, Chen *et al.* 2012, Dang *et al.* 2017, Ma *et al.* 2017, Michael *et al.* 2012, Tsonos 2008). Numerous researcher shown that bonding CFRP sheets method could significantly improve the seismic performance of the beam-column joints. However, for bonding CFRP sheets retrofitting method, the retrofitting effect is not as well as we thought. As we all know, bonding the CFRP sheets retrofitting method is a passive retrofitting method. In other words, the CFRP sheets will confine the concrete only concrete expended at the transverse direction, if there is no transverse deformation occurred, the CFRP sheets will not provide confinement on concrete.

To achieve a better confinement to concrete, many active retrofitting methods are also put forward, including prestressed steel wire rope method (Huang *et al.* 2015, Wu *et al.* 2010, 2014), prestressed FRP reinforcement method (Abdullah and Bailey 2018, Mazaheripour *et al*. 2016, Shayanfar and Bengar 2018) and shape memory alloy stirrup reinforcement method (Elbahy *et al*. 2010, Youssef and Nehdi 2008, Rezaee 2018). Based on those above active retrofitting methods, prestressed steel strips

*Corresponding author, Ph.D. Candidate
E-mail: xauatchenyang@126.com

ISSN: 2092-7614 (Print), 2092-7622 (Online)

Table 1 Specimen parameters

Series	Specimen No.	Axial compression ratio	Steel strips in beam end		Steel strips in joint core		Joint type
			Spacing	Layer	Spacing	Layer	
1	J-Q-1	0.3	—	—	—	—	Plane strong joint
	PSJ-Q-1	0.3	100	2	50	2	Plane strong joint
	PSJ-Q-2	0.3	100	4	50	2	Plane strong joint
	PSJ-Q-3	0.3	100	2	100	2	Plane strong joint
	PSJ-Q-4	0.3	100	2	100	2	Space strong joint
	CFRP-1	0.3	—	—	—	—	Space strong joint
2	J-R-1	0.2	—	—	—	—	Plane weak joint
	J-R-2	0.1	—	—	—	—	Plane weak joint
	PSJ-R-1	0.2	100	1	100	1	Plane weak joint
	PSJ-R-2	0.2	50	3	50	3	Plane weak joint
	PSJ-R-3	0.1	50	3	50	3	Plane weak joint

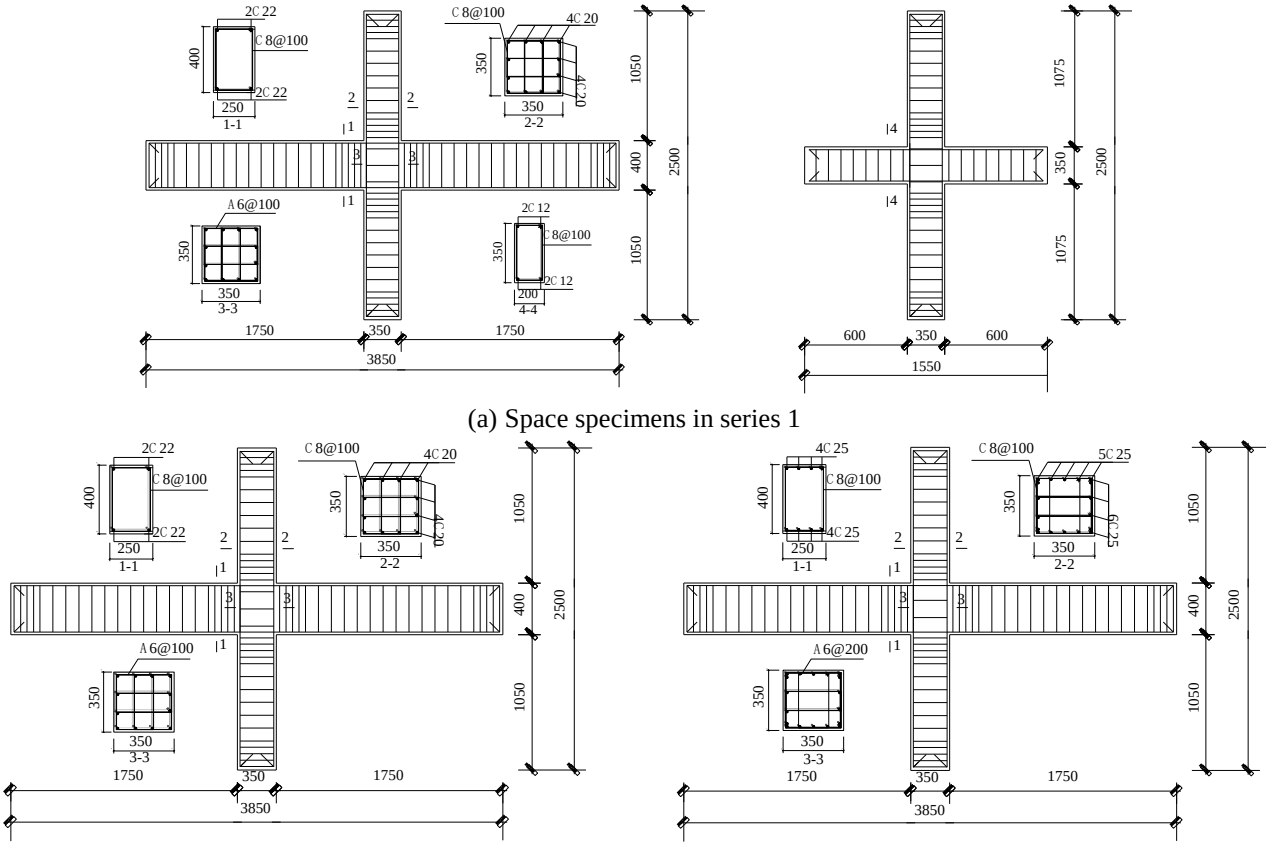

(a) Space specimens in series 1

(b) Plane specimens in series 1

(c) Specimens in series 2

Fig. 1 Cross section and reinforcement details of the specimens

retrofitting approach was proposed by Yong Yang. Over the last few years, a vast amount of researches had been carried out on prestressed steel strips retrofit of the reinforced concrete members, such as columns (Yang 2013, Zhang *et al.* 2015, 2016) and beams (Liu *et al.* 2013, 2015, Wang *et al.* 2015), all indicating the feasibility and the effectiveness of this retrofitting technique. Meanwhile, a set of design methods for predicting the strength of the retrofitted beams and columns were established. In this paper, in order to evaluate the seismic performance of prestressed steel strips reinforced beam-column joints, eleven specimens were conducted through quasi-static test. Furthermore, the failure modes, hysteresis response, stiffness, energy dissipation capacity and the damage level of the joint specimens were emphatically investigated.

2. Test program

2.1 Test specimens

In the experiment, a total of eleven beam-column joint specimens were manufactured and tested. The joint specimens were divided into two series according to the

Table 2 Tested mechanical properties

Type of the steel	Diameter /Thickness (mm)	Yield strength (MPa)	Ultimate strength (MPa)	Elastic modulus (GPa)
HPB300	6	389.2	578.3	205
HRB400	8	430.1	676.7	201
HRB400	20	451.7	603.3	223
HRB400	22	424.7	592.3	205
HRB400	25	435.2	607.5	206
Steel strips	0.9	770.7	877.4	184
CFRP	0.167	—	3300.0	240

type of the joint. The six specimens in series 1 were designed as strong beam-column joints, whereas the five specimens in series 2 were designed as weak beam-column joints. In general, bearing capacity of the core of the strong joint is higher than that of the beams and columns connected with it, and consequently the failure of the beam occurs prior to that of the joint core. Nevertheless, the weak joint is opposite. The strength grade of the concrete for two series of joint specimens was identical and designed as C25, the average cubic compression strength of concrete in both series was 33.3 MPa. For all plane joint specimens, the frame column had a cross section of 350 mm×350 mm, and the frame beam had a cross section of 250 mm×400 mm. The main parameters in two series are shown in Table 1. The dimensions and the details of the reinforcement are shown in Fig. 1.

In series 1, the axial compression ratios of columns were constant and designed as 0.3. The first specimen labeled as J-Q-1 is the control specimen that without retrofitting. Specimens labeled as PSJ-Q-1, PSJ-Q-2, PSJ-Q-3 and PSJ-Q-4 are retrofitted with prestressed steel strips, and specimen labeled as CFRP-1 is retrofitted with CFRP sheets for comparison with specimen PSJ-Q-4. Among these six specimens, two specimens PSJ-Q-4 and CFRP-1 are the space beam-column joints, while the other four specimens are plane beam-column joints. The cross section of secondary beam is 200 mm×350 mm in space joint specimens. The tested mechanical properties of the steel bars, prestressed steel strips and CFRP sheets are listed in Table 2.

In series 2, the axial compression ratios of columns were designed as 0.1 and 0.2. The specimen labeled as J-R-1 and J-R-2 are the control specimens, which were not retrofitted. Specimens labeled as PSJ-R-1, PSJ-R-2 and PSJ-R-3 are retrofitted with prestressed steel strips. In order to achieve the purpose of shear failure occurred in joint core, these specimens were designed according to principles of "strong component and weak joint".

For beam-column joints retrofitted with prestressed steel strips, the retrofitting steps were the same. First of all, before pouring the concrete, the corners in joint core and in its adjacent beam end and column end were beveled to round corners with PVC pipes to smooth the surface and reduce the effect of the friction, which were aimed to produce the consistent constraining force on the concrete with steel strips. The radius of all the rounded corners were 50 mm. Secondly, a set of rectangular steel tubes wrapping

(a) Steel strips

(b) Air compressor

(c) Stretching machine

(d)Steel strips connectors

Fig. 2 Retrofitting devices and stuff

(a) Reserved holes

(b) Twining steel strips

(c) Stretching steel strips

(d) Sealing the holes

Fig. 3 Progress of prestressed steel strips strengthened the beam-column joint

the white foam film were embedded at the end of the beam adjacent to the joint core, with an aim of removing the steel tubes smoothly. Thirdly, a set of steel strips were attached on the joint core and along the beam end and column end with a cantilever length of 400 mm, then stretching the steel strips with a stretching machine and anchoring them with steel strips connectors. Fig. 2 shows the retrofitting devices and stuff. The thickness and width of the steel strips are 0.9 mm and 50 mm, respectively. Because the steel strips were stretched before fixed, the prestress force were produced and were kept in the steel strips. By measuring and recording the strains of the steel strips in the retrofitted specimens, the measured average pre-strains of the steel strips were 433$\mu\varepsilon$, which meant that the prestress force of the steel strips were about 80 MPa. Finally, using the highly performance construction structural adhesives to seal the holes when the construction of the steel strips was completed. The progress of the prestressed steel strips method is shown in Fig. 3. Similarly, for existing joints that need retrofitting with steel strips in practical engineering application, it is necessary to bore some holes with

Fig. 4 Photo of joint retrofitted with steel strips

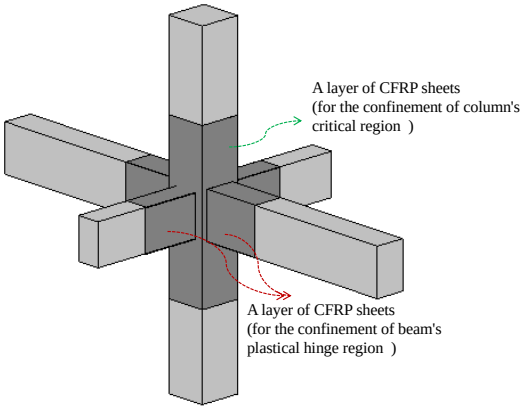

Fig. 5 Arrangement of the CFRP sheets

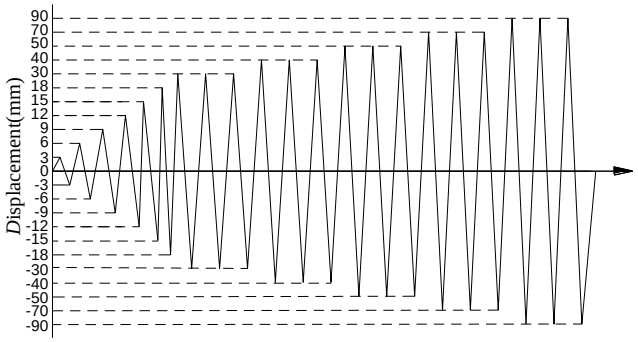

Fig. 6 Loading protocol of the test

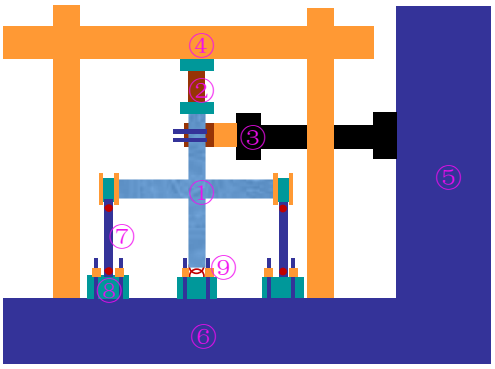

Fig. 7 Schematic diagram of test setup: ① joint specimen, ② vertical hydraulic jack, ③ hydraulic actuator, ④ crossbeam, ⑤ reaction wall, ⑥ lab ground, ⑦ tie rod, ⑧ bottom compression beam, ⑨ ball hinge

punching device firstly and grout the holes with mortar at last, the other reinforced steps are the same as described above. Fig. 4 presents a typical example of joint reinforced with prestressed steel strips in Xi'an, which shows that this method is effective and practical.

For specimen CFRP-1 retrofitted with a lay of CFRP sheet, the retrofit design was performed according to the retrofitting guideline developed by Italian National research Council, CNR-DT 200 (CNR-DT 2004). The CFRP sheets were formed from a layer of CFRP sheet with the thickness of 0.167 mm. As presented in Fig. 5, the length of the CFRP sheets was kept constant as 300 mm in two column ends, two frame beam ends and two secondary beam ends adjacent to the body of the joint, respectively.

2.2 Test setup and procedure

The tests were conducted in Structural Engineering Key Laboratory at Xi'an University of Architecture and Technology. All the specimens were tested under horizontal loading to simulate the seismic actions. As shown in Fig. 7, the vertical load was applied to the top of the upper column by means of the MTS electro-hydraulic servo actuators to simulate the *P*-Δ effect, both the beam ends were fixed through the tie rods connected to the bottom compression beam, with an aim of avoiding the vertical movement of the beam ends. To simulate the null flexural moment at mid-height of the entire column in a real frame under horizontal seismic effects, both the column ends were hinged using roller plates. In series 1, the constant axial load of 918.75 kN was applied to the upper column end using a stable pressure hydraulic jack and the load was measured using an electrical load cell, whereas in series 2, the magnitude of the axial force was determined by the different axial compression ratio.

In order to obtain the seismic requirements and capacities of the structure from quasi-static cyclic loading tests, establishing loading history that can simulate the actual seismic response is needed. It is well known that every excursion in the inelastic range results in cumulative damage in the structural elements and the strength and deformability of the structure mainly depend on its cumulative damage, which means that as the number of damaging cycles and the amplitude of cycling increase, the performance of the structure is tend to deteriorate gradually. In the utilized loading protocol, the repetition of the inelastic excursions per loading step is highlighted. Meanwhile, large inelastic excursions can bring about the large damage and consequently lead to the ultimate states of the structure (Karayannis *et al.* 1998, 2008, Tsonos 2007). Therefore, a loading protocol controlled by the displacement was adopted in the test. As plotted in Fig. 6, before the specimen yielded, the MTS actuator reversely loaded one cycle for each loading step. And after yielding, the displacement was reversely loaded and repeated three cycles for each loading steps. It was not until the horizontal load decreased to less than 85% of the peak load that the tests ended.

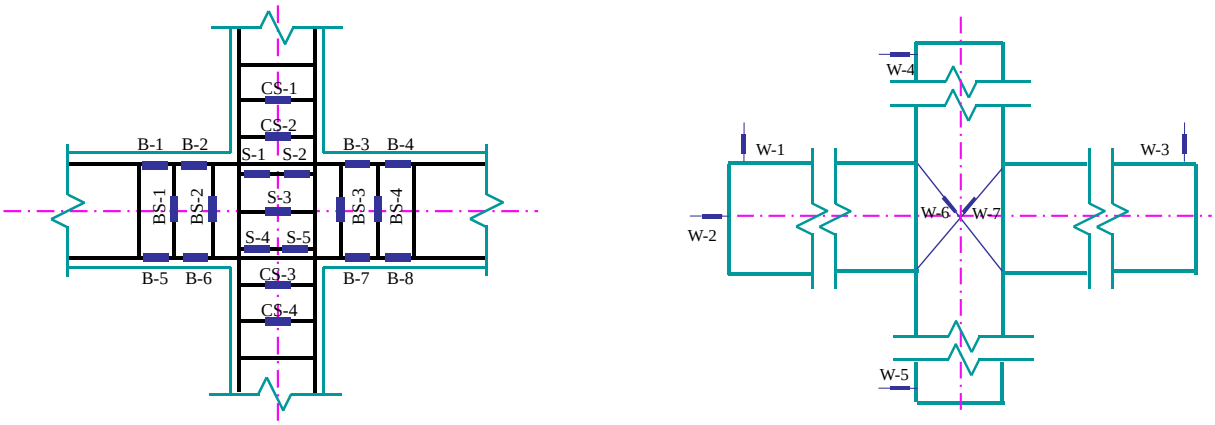

(a) Layout of the strain gauges (b) Layout of the LVDTs

Fig. 8 Layout of the LVDTs and strain gauges

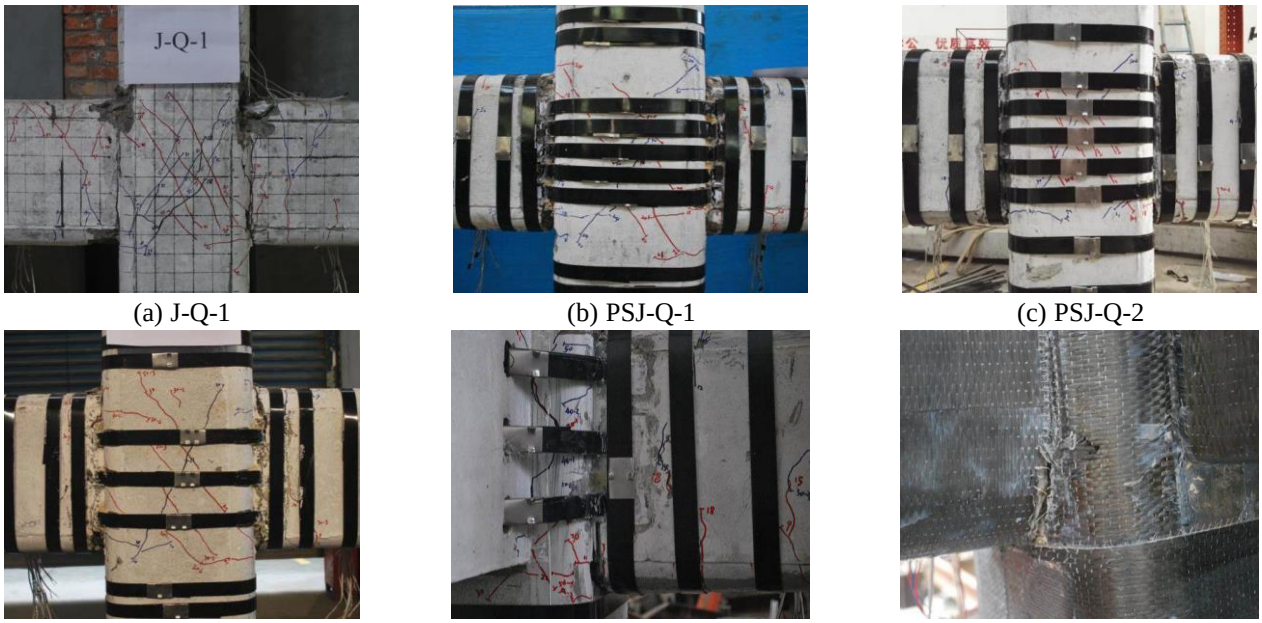

(a) J-Q-1 (b) PSJ-Q-1 (c) PSJ-Q-2

(d) PSJ-Q-3 (e) PSJ-Q-4 (f) CFRP-1

Fig. 9 Failure modes of the specimens

During the test, several strain gauges were used to monitor the response of the reinforcement in the joint. The layout of the strain gauges is plotted in Fig. 8(a), and the details of the displacement transducers (LVDTs) is illustrated in Fig. 5(b), where 3 transducers (W1-W3) were utilized to measure the beam response and 2 transducers(W4-W5) to measure the displacement of the column, as well as two line variable displacement transducers(W6-W7) to measure the shear deformation of the core of the joint.

3. Experimental results and discussions

3.1 Failure modes in series 1

3.1.1 Unretrofitted specimen

The failure mode of the specimen J-Q-1 is presented in Fig. 9(a). For specimen J-Q-1, when the top horizontal displacement reached 6 mm, the vertical bending cracks occurred on the tension side of the beam adjacent to the joint region. When the horizontal displacement was up to 18 mm, diagonal shear cracks appeared in the joint area and more and more bending cracks appeared in the beam end. Moreover, the strain of the longitudinal reinforcement of beam reached 1995 $\mu\varepsilon$ and the specimen yielded. With the horizontal displacement increasing, the *X* shaped diagonal crack in the joint region was developed and widened quickly, and bending cracks gradually continued to elongate along the beam height direction. Finally, the top concrete crushing at the beam adjacent to the joint area and the *X* shaped diagonal crack were observed. Therefore, the final failure mode of the unretrofitted specimen was a combination of flexural failure of beam and shear failure of joint core.

3.1.2 Specimen retrofitted with prestressed steel strips

The failure modes of the specimens PSJ-Q-1, PSJ-Q-2, PSJ-Q-3 and PSJ-Q-4 retrofitted by prestressed steel strips were found to be similar. Here just the failure progress of the specimen PSJ-S-1 were described. When the top horizontal displacement was 6 mm, the first bending crack appeared in the right beam adjacent to the joint area and no visible crack was observed in the joint core. When the horizontal displacement was up to 21 mm, some diagonal cracks with small width and length occurred in the joint area and the reinforcement strain of the frame beam reached 2990$\mu\varepsilon$, the specimen yielded. With the test going on, the diagonal crack extended and developed, the steel strips became more and more tight and the strain of the steel strips increased sharply, and some obvious sound of the steel strips were heard. When the horizontal displacement reached 40 mm, the bending cracks widened and developed quickly, but there is no further diagonal crack appeared in the joint region. When the horizontal displacement was up to about 90 mm, the width of the bending crack was close to 5mm, spalling of the concrete on the compression side of the beam adjacent to the joint region was also observed. As shown in Figs. 9(b)-(e), the final failure modes of the specimens retrofitted with prestressed steel strips were the flexural failure of the beam.

3.1.3 Specimen retrofitted with CRFP sheets

The failure progress of the specimen CFRP-1 retrofitted with the CFRP sheets was similar to that of the specimens retrofitted with prestressed steel strips. At the initial loading stage, the horizontal displacement was small, the crack development could not be observed in the joint core region and in the beam and column ends adjacent to the core area due to the wrapped CFRP sheets. When the horizontal displacement was 15 mm, some obvious sound of the CFRP sheets was heard, and some folds appeared in the CFRP sheet. Meanwhile, a number of vertical bending cracks occurred in the main beam adjacent to the joint area. As the horizontal displacement increased, the bending cracks developed and widened, and the CFRP sheets started to be broken. When the horizontal displacement reached 70 mm, some CFRP sheets were peeled off from the surface of the main beam. As shown ins Fig. 9(f), the final failure mode of the specimen CFRP-1 was the flexural failure of the beam.

3.2 Failure mode in series 2

3.2.1 Unretrofitted specimen

The failure modes of the specimens J-R-1 and J-R-2 are similar and presented in Figs. 10(a)-(b). For specimen J-R-1, the vertical load 815 kN was applied to the top of the column. When the top horizontal displacement reached 4 mm, a tiny vertical bending crack occurred on the tension side of the beam adjacent to the joint region. When the horizontal displacement was up to 12 mm, diagonal shear cracks appeared in the corner of the joint area. When the horizontal displacement reached 16 mm, bending cracks gradually stretched and the *X*-shaped diagonal crack in the joint region was formed and developed quickly. When the horizontal displacement was up to about 40 mm, the stirrups of the joint yielded, the length and width of the *X*-shaped diagonal cracks were increasing, but the bending cracks did not continue to develop as the displacement increasing. Finally, the concrete crushing at the joint area and the widen *X* shaped diagonal crack were observed. Therefore, the final failure mode of the unretrofitted specimen was the shear failure of joint core.

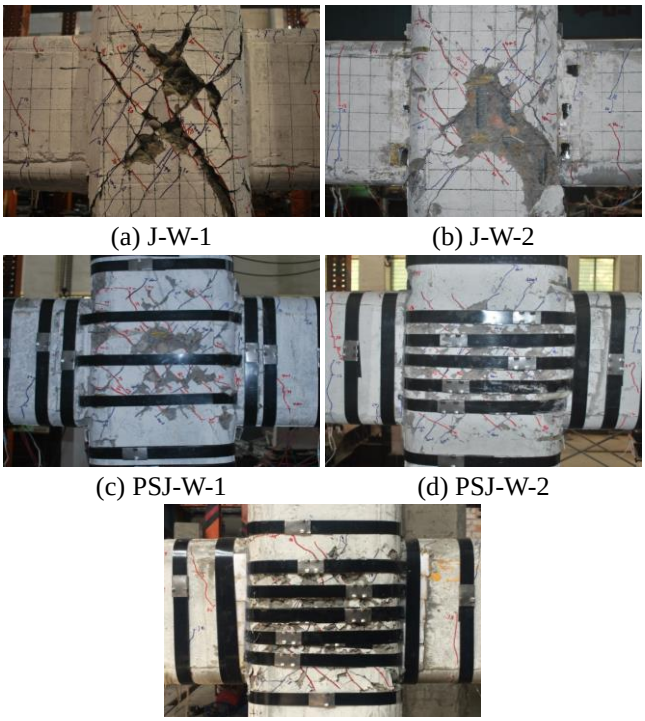

(a) J-W-1 (b) J-W-2

(c) PSJ-W-1 (d) PSJ-W-2

(e) PSJ-W-3

Fig. 10 Failure modes of the specimens in series 2

3.2.2 Retrofitted specimen

The failure modes of the retrofitted specimens PSJ-R-1, PSJ-R-2 and PSJ-R-3 were found to be similar. Here just the failure progress of the specimen PSJ-R-1 were described. When the top horizontal displacement was 9 mm, the first bending crack appeared in the beam adjacent to the joint area. When the horizontal displacement was up to 12 mm, some tiny diagonal cracks with small width and length occurred in the joint area. With the test going on, the diagonal crack gradually extended and developed in joint core. When the horizontal displacement reached 40mm, specimen started to yield. Furthermore, the diagonal cracks widened quickly, but the bending cracks developed slowly. When the horizontal displacement was up to about 60mm, the specimen reached the peak load and the slight spalling of the concrete in the joint region was observed. As the displacement increasing, the concrete in joint core continued to fall off, and when the displacement was up to 120 mm, the specimen reached the ultimate stage, the test was over. As shown in Figs. 10(c)-(e), the final failure modes of the specimens retrofitted with prestressed steel strips were also the shear failure of the joint core. However, compared with the specimen without retrofitting, the specimen retrofitted with prestressed steel strips had a significant improvement in bearing capacity and ultimate displacement. Moreover, the final cracks were more uniform and finer in ultimate stage, and the concrete

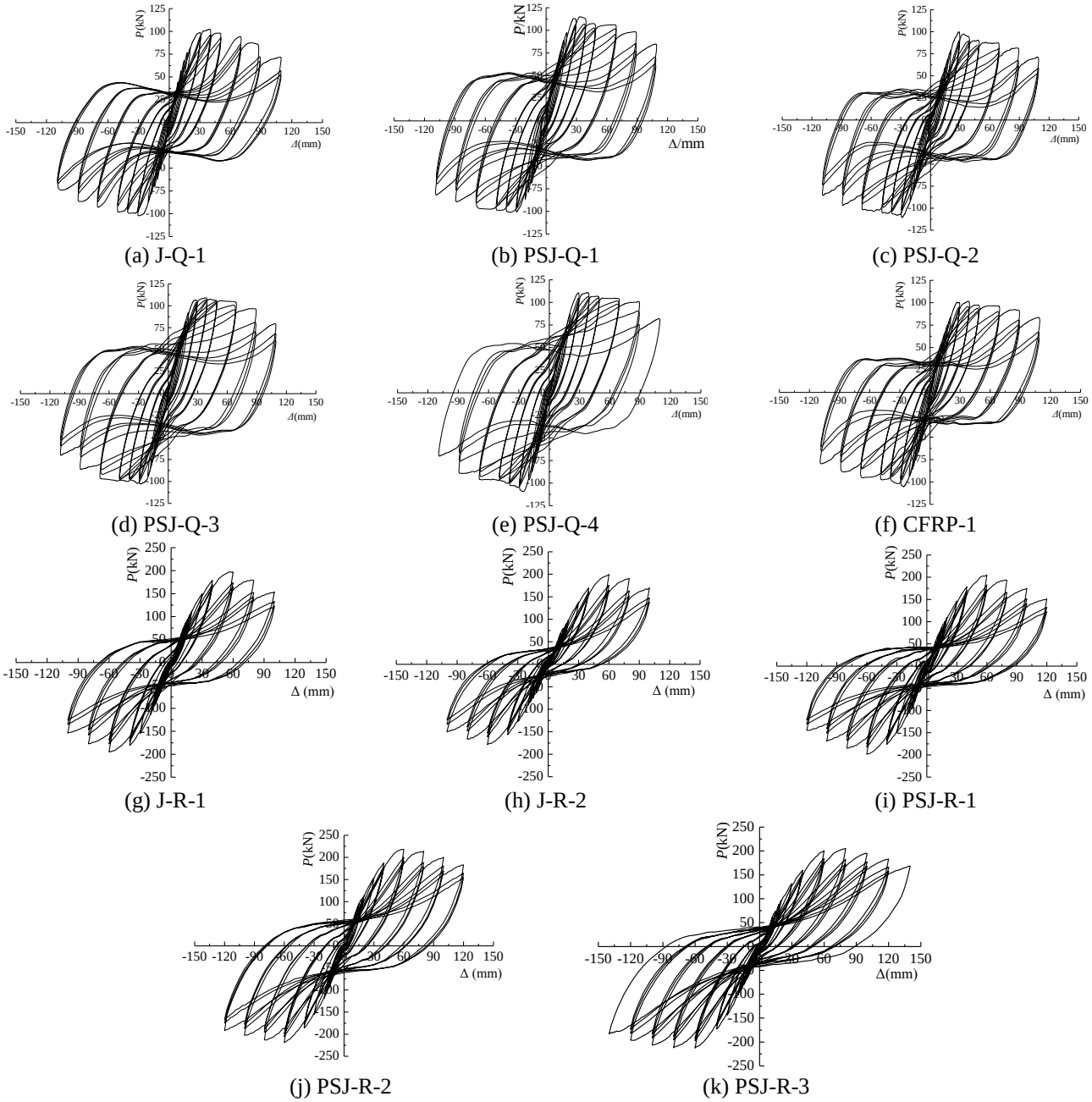

(a) J-Q-1 (b) PSJ-Q-1 (c) PSJ-Q-2

(d) PSJ-Q-3 (e) PSJ-Q-4 (f) CFRP-1

(g) J-R-1 (h) J-R-2 (i) PSJ-R-1

(j) PSJ-R-2 (k) PSJ-R-3

Fig. 11 Hysteresis curves of all the specimens

spalling in retrofitted joint core was less than that of unretrofitted specimen, so the integrity of the joint specimen retained well by retrofitting with prestressed steel strips.

3.3 Load-displacement hysteresis curves and skeleton curves

The relationship between the lateral load and displacement at the top of the column is presented by hysteresis curves, the hysteresis curves of all the specimens are illustrated in Fig. 11. Besides, the skeleton curves of each joint specimen for series 1 and series 2 obtained from the above load-deformation hysteresis curves are plotted in Fig. 12.

From Figs. 11-12, it can be seen that the areas of the hysteresis curves of the unstrengthened specimens are smaller than that of strengthened specimens, which indicates that the hysteresis behavior of the strengthened specimen is better than that of the unstrengthened specimen. Moreover, from the hysteresis curves of specimens of PSJ-Q-1, PSJ-Q-2 and PSJ-Q-3 in series 1, it can be concluded that the bearing capacity and the energy dissipation capacity increase with the increasing of the amount of the prestressed steel strips. Same conclusions can be obtained from the test results of specimens PSJ-R-1 and PSJ-R-2 in series 2. Therefore, prestressed steel strips retrofitting method can improve the seismic behavior of the RC beam-column joints. Furthermore, compared with the specimen J-R-2 with an axial compression ratio 0.1, the hysteresis

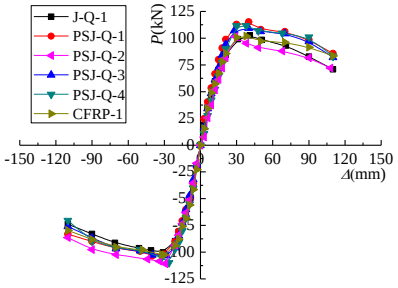

(a) Series 1

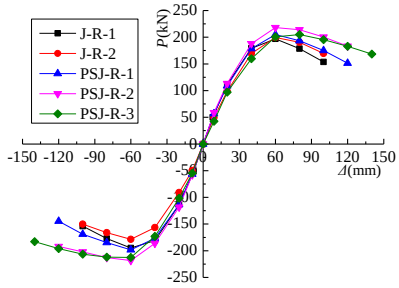

(b) Series 2

Fig. 12 Skeleton curves of specimens

curve of the specimen J-R-1 with an axial compression ratio 0.2 is more plumper. Therefore, increasing the axial compression ratio could get higher hysteresis performance of the joint specimens.

Fig. 13 illustrates the lateral displacements versus stirrup strains curves, which demonstrates that the stirrups in core of the joint yield and the stirrup strains of the unstrengthened specimens are larger than that of strengthened specimens. Because the prestressed steel strips could provide circumferential constraint on the joint core, the shear deformation of the joint core of the strengthened specimen can be effectively reduced and the strain of stirrups also greatly decrease. In the meanwhile, Fig. 14 plots the relationships between the nominal principal tensile stresses and the displacements in core regions of the joints. From Fig. 14, it can be observed the values of nominal principal tensile stress of the joint in specimen PSJ-Q-4 are slightly higher than those of the specimen CFRP-1. In addition, the values of the nominal principal tensile stress of specimens retrofitted with prestressed steel strips are higher than that of the control specimens, and increasing the

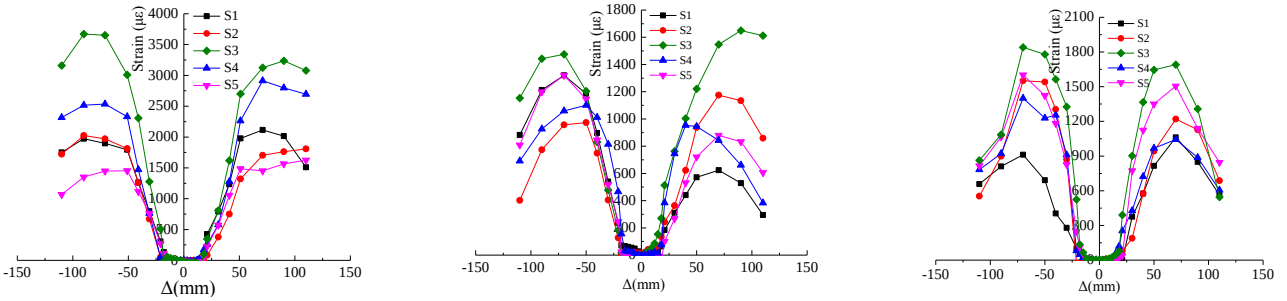

(a) J-Q-1 (b) PSJ-Q-1 (c) PSJ-Q-2

(d)J-R-1 (e) PSJ-R-2 (f) PSJ-R-3

Fig. 13 Curves of load versus stirrup strain

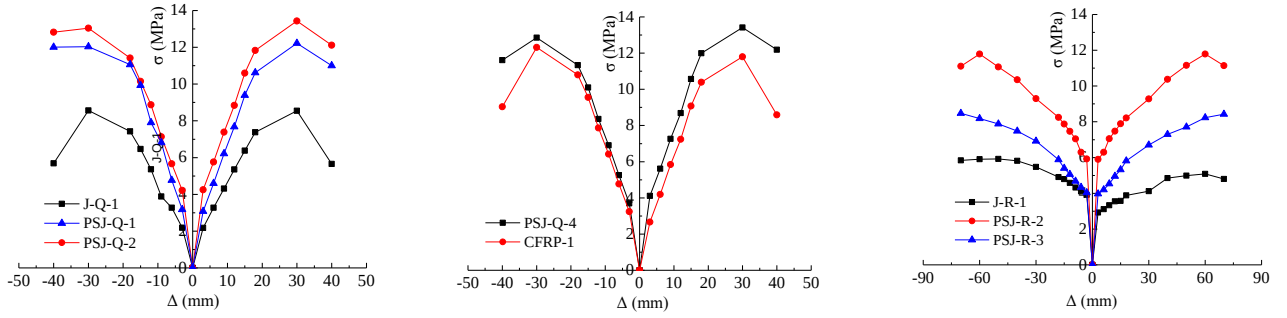

(a) J-Q-1, PSJ-Q-1 and PSJ-Q-2 (b) PSJ-Q-4 and CFRP-1 (c) J-R-1, PSJ-R-2 and PSJ-R-3

Fig. 14 Nominal principal tensile stress in core of the joint

Table 3 Main test results

Series	Specimen No.	P_y /kN	Imp. (%)	Δ_y /mm	P_m /kN	Imp. (%)	Δ_u /mm	$\mu=\Delta_u/\Delta_y$
1	J-Q-1	75.89	—	21.26	101.09	—	89.75	4.22
	PSJ-Q-1	90.38	19.09	19.51	108.31	7.14	96.00	4.92
	PSJ-Q-2	95.61	25.98	22.13	108.17	7.00	96.39	4.36
	PSJ-Q-3	78.61	3.58	17.63	106.34	5.19	91.35	5.18
	PSJ-Q-4	99.75	11.69	23.66	110.77	8.32	87.05	3.68
	CFRP-1	89.31	—	24.18	102.26	—	96.62	4.0
2	J-R-1	177.20	2.83	38.78	195.89	3.59	89.77	2.31
	J-R-2	172.32	—	42.12	189.10	—	99.90	2.37
	PSJ-R-1	181.30	2.31	41.52	201.78	7.60	100.55	2.42
	PSJ-R-2	195.78	10.47	43.49	218.20	11.39	121.79	2.80
	PSJ-R-3	187.59	8.86	48.78	208.88	10.46	137.04	2.83

amounts of the steel strips and decreasing the axial compression ratio can lead to a increasing of the nominal principal tensile stress of the joint core.

3.4 Strength and ductility

The values of the yield load P_y, yield displacement Δ_y, peak load P_m, ultimate displacement Δ_u, and the ductility coefficient μ of all specimens are listed in Table 3. In Table 3, imp. denotes the improvement rate of the yield load P_y and peak load P_m. From Table 3, some conclusions can be drawn as follow. Firstly, the bearing capacity of the retrofitted specimens was higher than that of the unretrofitted specimens, because the prestressed steel strips provided the confinement to the concrete. In series 1, the yield load and peak load of specimen PSJ-Q-2 were 95.61 kN and 108.17 kN, while those of the control specimen J-Q-1 were 75.89 kN and 101.09 kN, the yield load and peak load improved 25.98% and 7.00%, respectively. Similarly, from the results of the specimens J-R-1, PSJ-R-1 and PSJ-R-2 in series 2, it can be also concluded that the prestressed steel strips contributed well in bearing capacity of the joint specimens. Secondly, considering the retrofitted joint specimens PSJ-Q-1, PSJ-Q-2, PSJ-Q-3 failed in bending failure of beam, the ultimate load of the specimens was controlled by the bending bearing capacity of the beam. Thus, the peak load of the specimens retrofitted with prestressed steel strips were almost same but larger than that of unretrofitted specimens. Thirdly, according to the results of the specimens J-R-1 and J-R-2, it can be founded that the bearing capacity of the joint specimens increased with the increasing of the axial compression ratio, but the deformation capacity was reduced due to the larger axial compression ratio. The same conclusion can be obtained from the test results of the specimens PSJ-R-2 and PSJ-R-3. The last, the shear capacity of the specimen PSJ-Q-4 strengthened with steel strips was higher than that of the specimen CFRP-1 reinforced with CFRP sheets, although the ductility of the specimen PSJ-Q-4 was a little smaller than that of the specimen CFRP-1. As a result, the shear capacity and deformation capacity of the joint reinforced with prestressed steel strips method could as good as that of the specimen retrofitted with CFRP sheet.

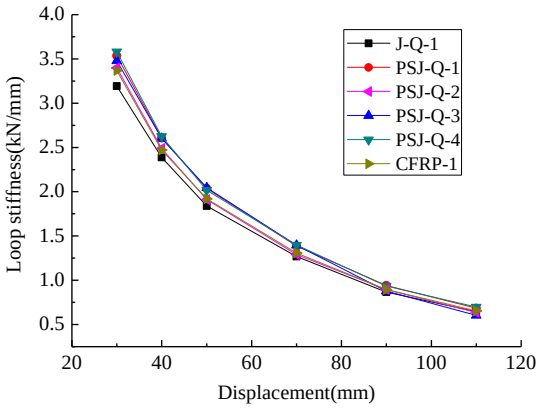

(a) Series 1

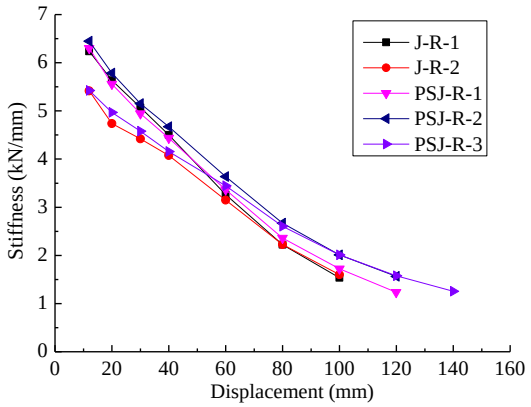

(b) Series 2

Fig. 15 Stiffness degradation of the specimens

3.5 Stiffness degradation

In the case of constant displacement amplitude, the stiffness of structural members subjected to cyclic loading decreases with the increase of loading times. Here the loop stiffness K_i is utilized to evaluate the stiffness degradation of the joint specimens, which is determined by following formula

$$K_i = \sum_{i=1}^{3} P_i / \sum_{i=1}^{3} \Delta_i \tag{1}$$

Where, P_i and Δ_i are the average peak load and displacement of the i-th loading step at the same displacement amplitude,respectively.

The stiffness degradation of all the joint specimens is presented in Fig. 15. From the Fig. 15, it can be observed that the stiffness of each specimen gradually degenerated with the increase of the horizontal displacement of the top column due to the concrete cracking during the loading progress. Meanwhile, as shown in Fig. 15(a), though the stiffness of the specimen CFRP-1 is slightly lower than that of the specimen PSJ-Q-4 in the test, the stiffness degradation rate of the specimens CFRP-1 retrofitted with CFRP sheets tends to be the same as that of the specimens PSJ-Q-4 retrofitted with prestressed steel strips. Additionally, as shown in Fig. 15(b), the stiffness

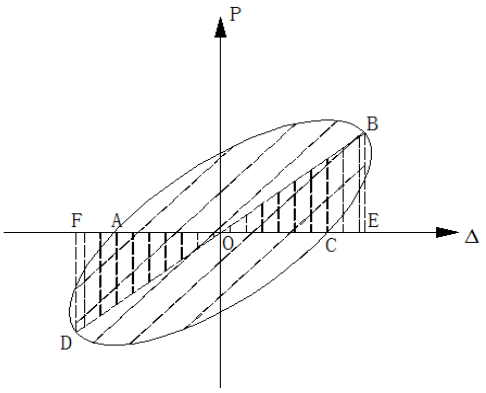

Fig. 16 The schematic of equivalent viscous damping coefficient

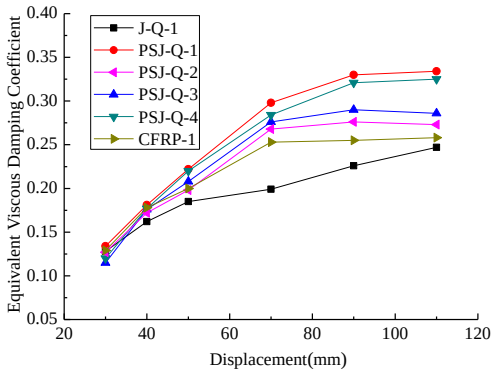

(a) Series 1

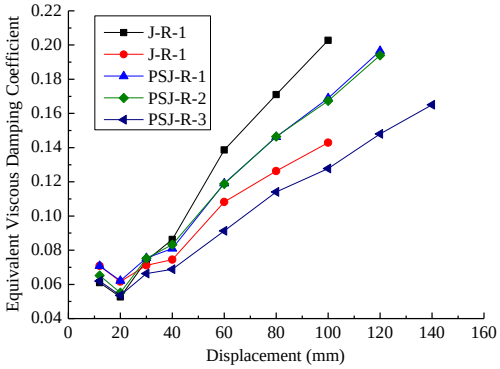

(b) Series 2

Fig. 17 Equivalent viscous damping coefficient

degradation of unstrengthened joint specimen J-R-1 is faster than that of the prestressed steel strips strengthened specimens. And for specimen with relative smaller axial compression ratio, the stiffness increases with the increasing of the axial compression ratio, but the stiffness degradation rate is fast as well.

3.6 Energy-dissipation behavior

Energy dissipation capacity is an important index to evaluate the seismic behavior of structure members. The higher energy-dissipation capacity is, the better the seismic behavior of the structure has. The energy consumption of all the specimens at different load step is listed in Table 4. For simplicity, the equivalent viscous damping coefficient he is

Table 4 Energy dissipation at different displacement in series 1

Specimen No.	Energy consumption value /(kN·m)						Total energy dissipation /(kN·m)	Improvement /%
	30	40	50	70	90	110		
J-Q-1	5.61	7.81	9.35	11.84	14.60	16.16	65.37	—
PSJ-Q-1	6.09	8.29	10.37	15.92	18.73	19.20	78.60	20.24
PSJ-Q-2	5.76	8.02	9.59	14.40	16.89	17.93	72.59	11.04
PSJ-Q-3	5.70	8.26	10.54	15.89	18.42	19.53	78.34	19.84
PSJ-Q-4	5.98	8.23	10.58	16.30	20.69	19.27	81.05	15.70
CFRP-1	5.65	7.66	9.48	14.18	15.94	17.14	70.05	—

adopted to calculate the energy dissipation capacity of the joint specimen and expressed as follows

$$h_e = \frac{1}{2\pi} \cdot \frac{S_{ABCDA}}{S_{\Delta OBE} + S_{\Delta ODF}} \tag{2}$$

Where, S_{ABCDA} denotes the area of the hysteresis loop ABCDA, $S_{\Delta OBE}$ and $S_{\Delta ODF}$ denote the area of the triangles OBE and ODF, as depicted in Fig. 16.

Fig. 17 illustrates the relationship of the equivalent viscous damping coefficient and the displacement. Seen from the Tables 4 and Fig. 17(a), it can be found that the equivalent viscous damping coefficient of prestressed steel strips retrofitted joint specimens in series 1 are larger than that of unretrofitted joint specimens. In the meantime, as shown in Table 5, the total energy dissipation of strengthened specimens in series 2 are higher than that of the unstrengthened specimen. It is deduced that the prestressed steel strips can significantly enhance the energy dissipation behavior of the joint specimens. In addition, the equivalent viscous damping coefficient and total energy consumption of specimen PSJ-Q-4 are higher than that of specimen CFRP-1. This demonstrates that the energy dissipation behavior of prestressed steel strips reinforced joint specimens in this test is superior to CFRP reinforced joint specimens. Also from the results, as shown in Table 5 and Fig. 17(b), the total energy dissipation of specimen PSJ-R-2 with an axial compression ratio of 0.2 is much higher than specimen PSJ-R-3 with an axial compression ratio of 0.1. Therefore, when the axial compression ration is relative smaller, increasing the axial compression ration can improve the energy dissipation performance of the beam-column joints.

3.7 Evaluation of the damage level

To evaluate the effectiveness of the prestressed steel strips rehabilitation techniques, the hysteretic performance and the characteristic points of the joint specimens without retrofitting are concerned and compared with those of the retrofitted specimens at the maximum load circle. In this study, a damage index model proposed by Park and Ang (1985) is recommended for the evaluation of the damage level of the specimens. This model is defined as a superposition of the damage issues from the maximum deformation and the dissipated energy under repeated cyclic loading, and it can be expressed as

Table 5 Energy dissipation at different displacement in series 2

Specimen No.	Energy consumption value/(kN·m)									Total energy dissipation/(kN·m)	Improvement /%
	12	20	30	40	60	80	100	120	140		
J-R-1	0.35	0.75	2.13	3.91	10.24	15.30	19.59	—	—	137.92	40.94
J-R-2	0.35	0.73	1.77	3.05	7.67	11.26	14.29	—	—	97.86	—
PSJ-R-1	0.40	0.87	2.11	3.61	9.05	13.88	18.25	21.92	—	183.43	33.00
PSJ-R-2	0.38	0.80	2.19	3.92	9.78	15.72	21.16	27.45	—	218.31	58.29
PSJ-R-3	0.31	0.67	1.72	2.88	7.13	11.97	16.16	21.16	25.51	188.10	92.21

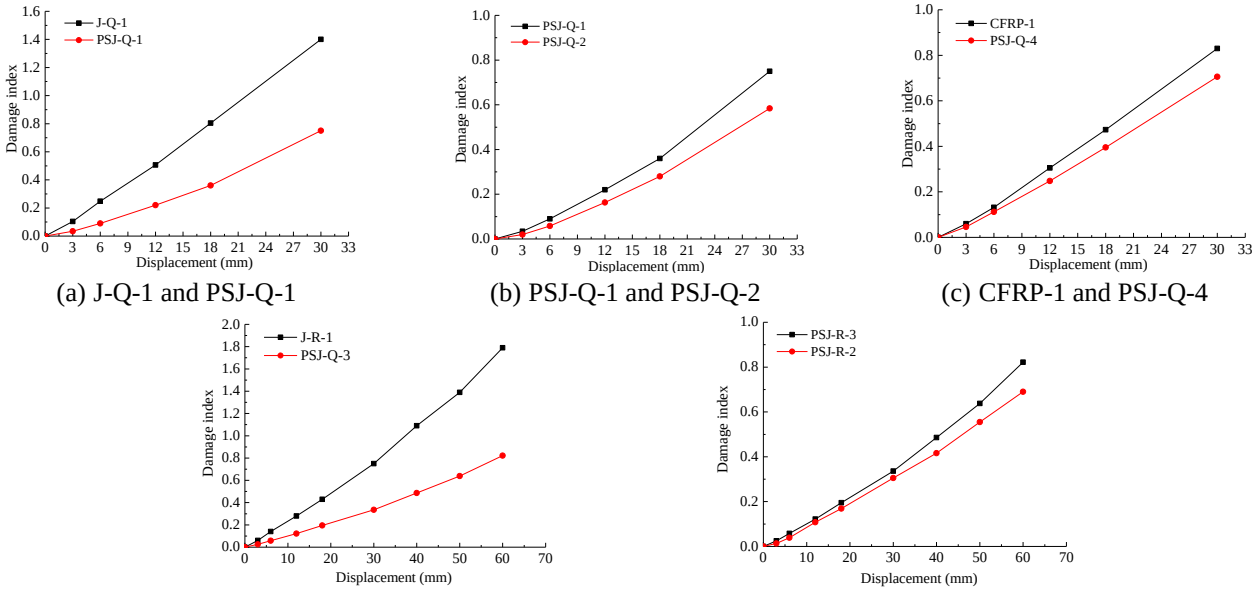

(a) J-Q-1 and PSJ-Q-1 (b) PSJ-Q-1 and PSJ-Q-2 (c) CFRP-1 and PSJ-Q-4

(d) J-R-1 and PSJ-R-2 (e) PSJ-R-2 and PSJ-R-3

Fig. 18 Comparison of the damage level

$$D=\frac{\delta_{\mathrm{m}}}{\delta_{\mathrm{u}}}+\frac{\beta}{Q_{\mathrm{y}}\delta_{\mathrm{u}}}\int dE \tag{3}$$

In which, δ_{m} is the maximum displacement under seismic loading, δ_{u} is the ultimate displacement under monotonic loading, β is a parameter related to the shear span ratio, axial stress, longitudinal reinforcement ratio and the lateral reinforcement ratio, Q_{y} is the yield strength, and dE is the incremental absorbed hysteretic energy.

In formula (3), the value of δ_{m}, Q_{y} and dE can be obtained from the experimental results. Nevertheless, the value of the δ_{u} can be estimated in accordance with Fardis and Biskinis (2003)

$$\delta_{\mathrm{u}}=\frac{1}{\gamma_{\mathrm{e1}}}0.016\times 0.3^{P^*}\left(\frac{\max(0.01,\omega')}{\max(0.01,\omega)}f_{\mathrm{cm}}\right)^{0.225}(L^*)^{0.35}25^{\alpha\rho} \tag{4}$$

In which, γ_{e1}=1.0, P^* denotes the axial compression ratio, ω and ω' denote the longitudinal reinforcement ratio of the reinforcement in tension and compression, respectively, f_{cm} denotes the compressive strength of the concrete, L^* denotes the shear span ratio, ρ_{s} denotes the ratio of transverse confinement steel to the volume of concrete core, α denotes the confinement effectiveness coefficient for rectangular hoops and can be determined from the Mander *et al.* (1986)

$$\alpha=(1-\sum_{i=1}^{n}\frac{(b_{\mathrm{i}})^2}{6b_{\mathrm{c}}d_{\mathrm{c}}}(1-\frac{s}{2b_{\mathrm{c}}})(1-\frac{s}{2d_{\mathrm{c}}}) \tag{5}$$

In which, b_{c} and d_{c} are the width and height of the concrete core section, respectively, s is the clear spacing of the hoops. Additionally, many researches have investigated about the value of β. As β=0.15 has been validated to be closed to the other damage model (Karayannis *et al.* 2008). For simplicity, 0.15 is also adopted in this study.

Fig. 18 shows the comparison of the damage index for different beam-column joints specimens. Fig. 18(a) and (d) present that the joint specimens strengthened with prestressed steel strips have a lower damage indexes in comparison with the control specimens. Fig. 18(b) and (e) present that increasing both the layer number of the steel strips and the axial compression ratio can reduce the damage index of the joint specimens. Besides, Fig. 18(c) demonstrates that the damage index of specimen retrofitted with prestressed steel strips rehabilitation method is slightly smaller than that of specimen retrofitted with CFRP sheets.

4. Conclusions

In this test, eleven beam-column joint specimens were conducted to investigate the effect of the prestressed steel strips on the joint seismic performance. Based on the

experimental results, some conclusions can be drawn as following

- The prestressed steel strips provided a substantial circumferential constraint on the concrete in strengthened specimens, it was helpful to postpone the emergence of the diagonal cracks of the joint core and improve the seismic performance of the joints. The prestressed steel strips method was proved to be an effective way to retrofit RC beam-column joints.
- For weak RC joint specimens, the failure mode of the unretrofitted joint specimen was a combination of the shear failure of the joint core and the bending failure of the beam, while the failure mode of the retrofitted specimens was bending failure of the beam. Consequently, ultimate bearing capacities of the plane joint specimens strengthened with prestressed steel strips were controlled by the bending capacity of the beam and their ultimate bearing capacity were almost the same.
- For strong RC joint specimens, the failure modes of all joint specimens were the shear failure of the joint core, but the concrete cracks in joint core were more finer and evenly after being strengthened, specimens exhibited higher bearing capacity, shear deformation capacity, energy dissipation capacity and ductility.
- The decrease of the spacing of the steel strips and the increase of the layer of the steel strips can greatly improve the bearing capacity, deformation capacity and energy dissipation capacity of RC beam-column joints. Furthermore, the bearing capacity, stiffness, equivalent viscous damping coefficient and energy dissipation performance of the joint specimens retrofitted with prestressed steel strips increased with the increasing of the axial compression ratio, but the ductility reduced as well.
- According to the comparing analysis, it could be found that the seismic behavior of the prestressed steel strips strengthened joint specimen was similar to and sometimes even better than that of the CFRP sheets strengthened joint specimen. In particular, from a cost-saving point of view, the prestressed steel strips will be more appropriate and economical than wrapping CFRP to retrofit the RC beam-column joints in engineering application.

Acknowledgements

The experiments were sponsored by National Research and Development Program of China (Program No. 2016YFC0701403), Research Project of Shaanxi Provincial Education Department (Program No. 14JF014) and also supported by the Program for Changjiang Scholars as well as the Program for Innovative Research Team of Xi'an University of Architecture and Technology.

References

Abdullah, A. and Bailey, C.G. (2018), "Punching behaviour of column-slab connection strengthened with non-prestressed or prestressed FRP plates", *Eng. Struct.*, **160**, 229-242.

Aiello, M.A. and Ombres, L. (2004), "Cracking and deformability analysis of reinforced concrete beams strengthened with externally bonded carbon fiber reinforced polymer sheets", *J. Mater. Civil Eng.*, **16**(5), 392-399.

Alemdar, F. and Sezen, H. (2010), "Shear behavior of exterior reinforced concrete beam-column joints", *Struct. Eng. Mech.*, **35**(1), 123-126.

Chen, W.W., Yeh, Y.K., Hwang, S.J., Lu, C.H. and Chen, C.C. (2012), "Out-of-plane seismic behavior and CFRP retrofitting of RC frames infilled with brick walls", *Eng. Struct.*, **34**(1), 213-224.

CNR-DT (2004), Istruzioni per la Progettazione, l'Esecuzione ed il Controllo di Interventi di Consolidamenti di Intervento Statico mediante l'utilizzo di Compositi Fibrorinforzati, CNR-DT.200/2004.

Colalillo, M.A. and Sheikh, S.A. (2012), "Seismic retrofit of shear-critical reinforced concrete beams using CFRP", *Constr. Build. Mater.*, **32**(7), 99-109.

Dang, H.V., Lee, D. and Lee, K. (2017), "Single and multi-material topology optimization of CFRP composites to retrofit beam-column connection", *Comput. Concrete*, **19**(4), 405-411.

Duan, H. and Hueste M.B.D. (2012), "Seismic performance of a reinforced concrete frame building in China", *Eng. Struct.*, **41**(3), 77-89.

Elbahy, Y.I.E.I., Youssef, M.A.Y.A. and Nehdi, M.N. (2010), "Deflection of superelastic shape memory alloy reinforced concrete beam", *Can. J. Civil. Eng.*, **37**(6), 842-854.

Fardis, M.N. and Biskinis, D.E. (2003), "Performance-based engineering for earthquake resistant reinforced concrete structures: a volume Honoring Shunsuke Otani", Deformation Capacity of RC Members, as Controlled by Flexure or Shear, Eds. Kabeyasawa, T. and Shiohara, H., University of Tokyo, Tokyo.

GB/T 50081-2010 (2010), *Standard for Test Method of Mechanical Properties on Ordinary Concrete*, China Planning Press, Beijing, China.

Guo, H.R. (2011), "The reliability of enlarging the cross-section in reinforcing the frame construction buildings", *Adv. Mater. Res.*, **189-193**, 4365-4369.

Han, C., Li, Q., Wang, X., Jiang, W. and Li, W. (2016), "Research on rotation capacity of the new precast concrete assemble beam-column joints", *Steel Compos. Struct.*, **22**(3), 613-625.

Hawileh, R.A., Rasheed, H.A., Abdalla, J.A. and Al-Tamimi, A.K. (2014), "Behavior of reinforced concrete beams strengthened with externally bonded hybrid fiber reinforced polymer systems", *Mater. Des.*, **53**(1), 972-982.

Huang, J., Zhu, C., Gong, Z. and Zhang, F. (2012), "Experimental study on seismic behavior of earthquake-damaged RC frame strengthened by enlarging cross-section", *Chin. Civil Eng. J.*, **45**(12), 9-17.

Huang, Q., Guo, Z., Cui, J., Yang, L. and University, H. (2015), "Experimental study on seismic behavior of RC frame joints strengthened with prestressed steel wire rope", *Chin. Civil Eng. J.*, **48**(6), 1-8.

Karayannis, C.G. and Sirkelis, G.M. (2010), "Strengthening and rehabilitation of RC beam-column joints using carbon-FRP jacketing and epoxy resin injection", *Earthq. Eng. Struct. Dyn.*, **37**(5), 769-790.

Karayannis, C.G., Chalioris, C.E. and Sideris, K.K. (1998), "Effectiveness of RC beam-column connection repair using epoxy resin injections", *J. Earthq. Eng.*, **2**(2), 217-240.

Karayannis, C.G., Chalioris, C.E. and Sirkelis, G.M. (2008), "Local retrofit of exterior RC beam-column joints using thin RC jackets-an experimental study", *Earthq. Eng. Struct. Dyn.*, **37**(5), 727-746.

Khalili, A., Kheyroddin, A., Emamee, E. and Sharbatdar, M.K.

(2016), "An innovative experimental method to upgrade performance of external weak RC joints using fused steel prop plus sheets", *Steel Compos. Struct.*, **21**(2), 443-460.

Lee, J. and Lopez, M.M. (2016), "Characterization of FRP Uwrap anchors for externally bonded FRP-reinforced concrete elements: an experimental study", *J. Compos. Constr.*, **20**(4), 04016012.

Li, B., Lam, S.S., Wu, B. and Wang, Y.Y. (2015), "Seismic behavior of reinforced concrete exterior beam-column joints strengthened by ferrocement composites", *Earthq. Struct.*, **9**(1), 233-256.

Liu, Y., Gao, Z., Lu, J., Yang, Y., Xue, J. and Sui, Y. (2013), "Experimental study on mechanical properties of reinforced concrete beams and columns confined by prestressing steel strip", *J. Build Struct.*, **34**(10), 120-127.

Liu, Y., Guo, L., Yang, Y., Tian, J. and Zhou, T. (2015), "Experimental study of shear performance of reinforced concrete beams retrofitted by prestressed steel strips", *Ind. Constr.*, **45**(3), 16-18+34.

Ma, C., Wang, D. and Wang, Z. (2017), "Seismic retrofitting of full-scale RC interior beam-column-slab subassemblies with CFRP wraps", *Compos. Struct.*, **159**, 397-409.

Mander, J.B., Priestley, M.J.N. and Park, R. (1988), "Theoretical stress-strain model for confined concrete", *J. Struct. Eng.*, **114**(8), 1804-1826.

Mazaheripour, H., Barros, J.A.O., Soltanzadeh, F. and Sena-Cruz, J. (2016), "Deflection and cracking behavior of SFRSCC beams reinforced with hybrid prestressed GFRP and steel reinforcements", *Eng. Struct.*, **125**, 546-565.

Men, J., Zhang, Y., Guo, Z. and Shi, Q. (2015), "Experimental research on seismic behavior of a composite RCS frame", *Steel Compos. Struct.*, **18**(4), 971-983.

Park, Y.J. and Ang, H.S. (1985), "Mechanistic seismic damage model for reinforced concrete", *J. Struct. Eng.*, **111**(4), 722-739.

Rezaee Azariani, H., Esfahani, M.R. and Shariatmadar, H. (2018), "Behavior of exterior concrete beam-column joints reinforced with Shape Memory Alloy (SMA) bars", *Steel Compos. Struct.*, **28**(1), 83-98.

Shan, C. (2012), "Calculation method of bending crack width in RC beams strengthened by bonding steel plate", *J. Southwest Jiaotong Univ.*, **45**(4), 508-513.

Shayanfar, J. and Bengar, H.A. (2018), "A practical model for simulating nonlinear behaviour of FRP strengthened RC beam-column joints", *Steel Compos. Struct.*, **28**(1), 49-74.

Thomsen, H.H. (2004), "Failure mode analysis of reinforced concrete beams strengthened in flexure with externally bonded fiber reinforced polymers", *J. Compos. Constr.*, **8**(2), 123-131.

Tsonos, A.D.G. (2010), "Performance enhancement of R/C building columns and beam-column joints through shotcrete jacketing", *Steel Constr.*, **32**(3), 726-740.

Tsonos, A.G. (2007), "Cyclic load behavior of reinforced concrete beam-column subassemblages of modern structures", *ACI Struct. J.*, **104**(4), 468-478.

Tsonos, A.G. (2008), "Effectiveness of CFRP-jackets and RC-jackets in post-earthquake and pre-earthquake retrofitting of beam-column subassemblages", *Eng. Struct.*, **30**(3), 777-793.

Wang, H., Yang, Y., Wang, A. and Liu, Y. (2015), "Experimental study of shear resistance of after-fire reinforced concrete t-shaped beam retrofitted with prestressed steel strips", *Ind. Constr.*, **45**(3), 22-28.

Wang, N., Ellingwood, B.R. and Zureick, A.H. (2010), "Reliability-based evaluation of flexural members strengthened with externally bonded fiber-reinforced polymer composites", *J. Struct. Eng.*, **136**(9), 1151-1160.

Wu, G., Jiang, J.B., Wu, Z.S., Tian, Y. and Zhang, M. (2010), "Experimental study of RC beams strengthened with distributed prestressed high-strength steel wire rope", *Mag. Concrete Res.*, **62**(4), 253-265.

Wu, G., Wu, Z., Wei, Y., Jiang, J. and Cui, Y. (2014), "Flexural strengthening of RC beams using distributed prestressed high strength steel wire rope: theoretical analysis", *Struct. Infrastr. Eng.*, **10**(2), 160-174.

Yang, Y. (2013), "Experimental study on reinforced concrete column retrofitted by prestressed steel strips", *Ind. Constr.*, **43**(2), 45-48.

Youssef, M.A. and Nehdi, M.S.A.M. (2008), "Experimental investigation on the seismic behavior of beam-column joints reinforced with superelastic shape memory alloys", *J. Earthq. Eng.*, **12**(7), 1205-1222.

Zgür Yurdakul, Ö. and Avşar, Ö. (2015), "Structural repairing of damaged reinforced concrete beam-column assemblies with CFRPs", *Struct. Eng. Mech.*, **54**(3), 521-543.

Zhang, B., Yang, Y., Wei, Y.F., Liu, R.Y., Ding, C. and Zhang, K.Q. (2015), "Experimental study on seismic behavior of reinforced concrete column retrofitted with prestressed steel strips", *Struct. Eng. Mech.*, **55**(6), 1139-1155.

Zhang, L., Ning, G., Li, J. and Yang, Y. (2016), "Experimental study of reinforced concrete columns strengthened by prestressed steel strips", *Ind. Constr.*, **46**(3), 155-159.

AT